



Radiation in 1.5 GeV and 12 GeV Laser Wakefield Acceleration Stages from PIC Simulations

J. L. Martins, S. F. Martins, R. A. Fonseca, and L. O. Silva

Citation: [AIP Conference Proceedings](#) **1299**, 191 (2010); doi: 10.1063/1.3520312

View online: <http://dx.doi.org/10.1063/1.3520312>

View Table of Contents: <http://scitation.aip.org/content/aip/proceeding/aipcp/1299?ver=pdfcov>

Published by the [AIP Publishing](#)

Articles you may be interested in

[Electron acceleration in cavitated laser produced ion channels](#)

Phys. Plasmas **20**, 103121 (2013); 10.1063/1.4825140

[Study of electron acceleration and x-ray radiation as a function of plasma density in capillary-guided laser wakefield accelerators](#)

Phys. Plasmas **20**, 083106 (2013); 10.1063/1.4817747

[Probing electron acceleration and x-ray emission in laser-plasma accelerators](#)

Phys. Plasmas **20**, 063101 (2013); 10.1063/1.4810791

[Betatron radiation from a beam driven plasma source](#)

AIP Conf. Proc. **1507**, 705 (2012); 10.1063/1.4773784

[GeV electron beams from a centimeter-scale channel guided laser wakefield accelerator](#)

Phys. Plasmas **14**, 056708 (2007); 10.1063/1.2718524

Radiation in 1.5 GeV and 12 GeV Laser Wakefield Acceleration Stages from PIC Simulations

J.L. Martins*, S.F. Martins*, R.A. Fonseca*,[†] and L.O. Silva*

*GoLP / Instituto de Plasmas e Fusão Nuclear - Laboratório Associado, Instituto Superior Técnico, Av. Rovisco Pais 1049-001, Lisboa, Portugal

[†]DCTI, ISCTE - Lisbon University Institute, Av. das Forças Armadas 1649-026, Lisboa, Portugal

Abstract. A massively parallel post-processing radiation diagnostic for PIC codes is presented, which is then used to study the main features of the radiation from single LWFA stages (1.5 GeV and 12 GeV). This diagnostic also allows to examine radiation signatures associated with the physics of self-injection.

Keywords: betatron radiation, PIC codes, laser wakefield acceleration

PACS: 52.38.Ph

INTRODUCTION

Particle-in-cell (PIC) codes have been widely used in the modeling of plasma-based accelerators since their first proposal by Tajima and Dawson [1]. Recently, a lot of interest has arisen in the application of plasma-based accelerators as sources of X-rays which can be emitted when the injected electrons undergo betatron oscillations (see for e.g. [2, 3, 4, 5, 6, 7, 8, 9]). However, the modeling of this radiation in PIC simulations presents some additional challenges.

PIC codes only capture radiation whose wavelength is resolved by the grid. The spatial scales involved in modeling plasma-based accelerators range from the laser wavelength, which is typically on the order of hundreds of nanometers, to the plasma skin depth, on the order of $10 - 10^2 \mu\text{m}$ (for plasma densities on the order of $10^{16} - 10^{19} \text{cm}^{-3}$), to the propagation length, which can reach several tens of cm. The X-ray radiation wavelength, on the other hand, ranges from 10 nm to 100 pm, order(s) of magnitude below the above mentioned length scales. This means that to capture this radiation in PIC codes a significant increase in resolution would be required, rendering multi-dimensional simulations computationally very demanding.

One of the ways to overcome this problem is to post-process the particle trajectories taken from the PIC simulations to determine the energy and spectrum of the radiation emitted by these particles. This technique allows the retrieval of the emitted radiation features while keeping the grid cell size, lessening the memory requirements. This method can be used to mimic experimental detectors, providing predictions for experimental measurements. Several diagnostics of this kind have been proposed (see e.g. [2, 10, 11, 12]). In this work we present a massively parallel post-processing diagnostic that takes the data of the particle trajectories in phase space from PIC simulations and determines the radiated energy and its spectral features in virtual detectors specified by the user [13].

This technique is general and can be used to assess the different radiative mechanisms taking place in laser-wakefield acceleration (LWFA) scenarios, from the radiation associated with the self-injection process, on the terahertz range [3], to the betatron radiation, which often reaches the X-ray regime.

This paper is structured in the following manner: in section 2 the radiation diagnostic we have implemented is described; in section 3, the radiation emitted by self-injected electron bunches in a 1.5 and a 12 GeV laser-wakefield stages is analyzed and finally in section 4 our conclusions are presented.

RADIATION DIAGNOSTIC

The radiation diagnostic we have implemented consists of two parts. In the first part of the diagnostic the spatially resolved radiated energy is calculated and deposited in a "virtual detector", which is simply a region of space specified by the user. The second part is responsible for determining the spectrum of the radiation in a region designated by the user.

The calculation of both the radiated energy and its spectrum requires the particle's trajectory in phase space. In the present work these data are obtained directly in the PIC simulations which were performed with the OSIRIS 2.0 framework [14], by saving the trajectories of particles of interest. The radiation diagnostic code is general though, and can be used with data from other sources as well, only requiring that data describing the trajectory are provided in a prescribed format.

In OSIRIS 2.0 particle tracking [15] is done in two steps. First, the simulation is run with tags attached to each particle (of the species of interest). With the data obtained in this simulation and using data mining tools, the particles of interest to the radiation calculation are then selected. In plasma-based accelerator scenarios, these are the electrons trapped inside the ion cavity region, also known as the bubble. A subset of these is usually selected to reduce the computational time. The exact same simulation is then run for a second time in which the trajectories in phase space of the selected particles are saved.

The calculation of the radiated energy into the "virtual detector" is done by cycling through the particles and determining the power they radiate into the center of each detector cell, which can be expressed as [16]:

$$\frac{dP}{dS} = \frac{e^2}{4\pi c} \frac{|\vec{n} \times [(\vec{n} - \vec{\beta}) \times \vec{\beta}]|^2}{(1 - \vec{\beta} \cdot \vec{n})^5 R(t')^2} \quad (1)$$

where P is the radiated power, dS is an infinitesimal element of area, e is the electron charge, c is the velocity of light, $\vec{\beta}$ is the velocity of the particle normalized to c , $R(t')$ is the distance from the particle position at the time of emission t' to the center of the detector cell and \vec{n} is a unit vector pointing from the particle position in the direction of the cell center. The radiated energy is then obtained by appropriately integrating dP/dS in time (for each time step) and in the space, over the detector cell surface.

The calculation of the radiation spectrum is done in a similar fashion. For each point in space where the spectrum is to be determined, the radiated energy per unit of frequency and per unit of area is obtained at each of the frequency axis points, according to [16]:

$$\frac{d^2 I}{d\omega dS} = \frac{e^2}{4\pi c} \left| \int_{-\infty}^{+\infty} \frac{\vec{n} \times [(\vec{n} - \vec{\beta}) \times \vec{\beta}]}{(1 - \vec{\beta} \cdot \vec{n})^2 R(t')} e^{i\omega(t' + R(t')/c)} dt' \right|^2, \quad (2)$$

where I is the radiated energy and $d\omega$ is an infinitesimal element of frequency. In the following we will often refer to the radiated energy per unit of frequency and per unit of area simply as spectrum.

When choosing the detector cell size care should be taken to properly resolve the region of space delimited by the radiation beaming angle since the energy is assumed to be constant inside each cell. In addition, the frequency resolution is dependent on the available time resolution of the particle trajectories. The diagnostic also enables the use of quadratic spline interpolation to increase the number of trajectory points per unit of time to extend the spectrum calculation up to higher frequencies with reduced noise.

BETRATRON RADIATION FROM A 1.5 GEV AND A 12 GEV SINGLE STAGE LASER-WAKEFIELD ACCELERATORS

1.5 GeV Single Stage Laser-Wakefield Accelerator

The diagnostic described in the previous section has been applied to numerous scenarios in plasma physics. Here we present results from a study of the betatron radiation emission in a 1.5 GeV self-injection single stage.

To illustrate a 1.5 GeV laser-wakefield accelerator stage a 3D simulation was performed where an 800 nm wavelength laser with a normalized peak vector potential of 4.0, a temporal width of 30 fs and a spot size of 19.5 μm was sent through a plasma with an electron density of $1.5 \times 10^{18} \text{cm}^{-3}$ and a propagation length of 0.75 cm. These parameters obey the matching conditions proposed in [17]. The simulation was performed in a boosted frame with a Lorentz factor of 5, since the use of Lorentz boosted frames in PIC simulations has been shown to provide a means of decreasing the run time [18, 19]. This technique is particularly useful in modeling long plasma-based accelerators given that the run time increases proportionally to the laser/beam propagation distance in conventional simulations. In the boosted frame the simulation box was $160 \times 32 \times 32 c/\omega_p$, where ω_p is the electron plasma frequency, with $2048 \times 256 \times 256$ cells, with the laser propagating in the x_1 direction.

From the self-injected electron bunch observed in the simulation, a sample of 1000 macroparticles was chosen (out of ~ 24000 self-injected electron macroparticles used in the simulation) and their trajectories recorded. A section of these trajectories is shown in Fig. 1(a), where both the betatron oscillations and the energy increase due to the longitudinal acceleration field inside the blowout region can be observed. The tracks go up to the 1.1 GeV accelerating stage. We note however that with this parameters they could reach the 1.5 GeV energy if the laser pulse was allowed to propagate up to a distance of 0.75 cm.

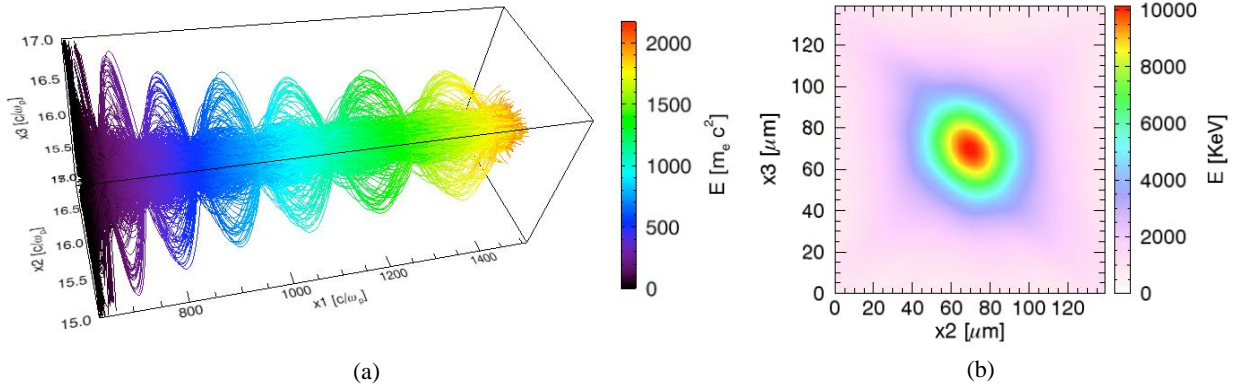


FIGURE 1. (a) Particle trajectories from the 1.5 GeV LWFA stage colored according to their kinetic energy; (b) energy deposited by the sample electrons at a detector placed about 2 cm away from the end of the trajectories.

The radiated energy of these electrons was determined on two square detectors placed 0.21 cm and 1.95 cm (Fig. 1(b)) away from the end of the particle trajectories. The full width at half maximum of a vertical and a horizontal lineouts passing at the center of the two radiated energy plots were recorded. Using this information the betatron radiation beam angular width was estimated to be ~ 2.3 mrad in the x_2 direction and ~ 2.2 mrad in the x_3 direction. Estimates of the radiation beam angular width based on the minimum and maximum values of the bunch electrons energy and of the amplitude of their oscillations pointed to a value in the range of ~ 5 to ~ 40 mrad. Since the radiated energy increases with the electron energy it is expected that the later part of the trajectories should contribute more to the beam angular aperture, which is in agreement with the fact that the measured value is on the order of the minimum value (obtained with the values taken at the end of the trajectories).

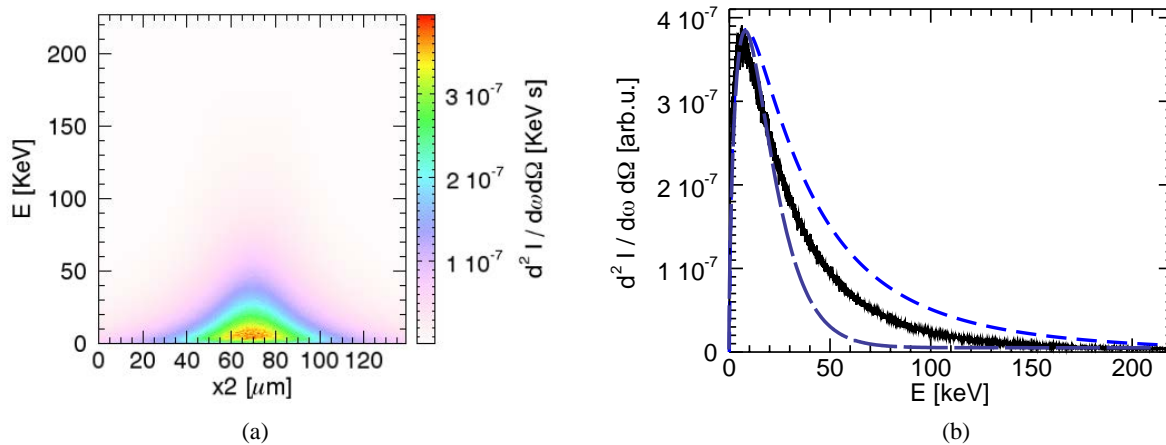


FIGURE 2. (a) The radiation spectrum per unit of solid angle and per unit of frequency in a horizontal line passing at the center of the virtual detector (depicted in Fig. 1(b)) is presented; (b) comparison of the on-axis spectrum (solid line) with a weighted average of the (synchrotron) asymptotic limit of the betatron radiation spectrum (short dash line) and with a pure synchrotron spectrum with the same peak position (long dash line).

The spectrum per unit of solid angle and per unit of frequency of the betatron radiation was also determined along a horizontal line passing through the detector center (Fig. 2(a)). The peak position of this spectrum was about 5 keV

which is well below the estimated critical energy value one obtains based on the maximum amplitude of oscillations at the end of the trajectories and the maximum electron energy, which would be ~ 40 keV. The particle trajectories show that, as expected, there is a distribution of amplitudes of oscillations and of energy for electrons at the same $x1$ position. This can influence the spectrum shape significantly. To confirm that the reason behind this discrepancy lies in the detailed composition of the electron bunch and on its acceleration over time, a comparison was made between the on-axis measured spectrum and a weighted average of an on-axis betatron spectrum theoretical formula. In the limit of $\gamma \gg 1$, where γ is the Lorentz relativistic factor of the electron, the on-axis betatron spectrum approaches a synchrotron-like shape [3]:

$$\frac{d^2\tilde{I}}{d\tilde{\omega}d\Omega} \sim \frac{1}{3}(\tilde{\omega}\tilde{\rho})^2\left(\frac{1}{\gamma^2} + \theta^2\right)^2\left(K_{2/3}^2(\xi) + \frac{\theta^2}{(1/\gamma^2) + \theta^2}K_{1/3}^2(\xi)\right) \quad (3)$$

where ξ is given by

$$\xi = \frac{\tilde{\omega}\tilde{\rho}}{3}\left(\frac{1}{\gamma^2} + \theta^2\right)^{3/2} \quad (4)$$

and the cyclotron radius is replaced by:

$$\tilde{\rho} = 2\gamma/r_0 \quad (5)$$

where r_0 is the amplitude of the betatron oscillation. To reflect the composition of the electron bunch and its evolution, this spectrum as weighted by all the pairs of $(r_{0max}(t), \gamma(t))$, throughout the whole trajectory of all the sample particles, where $r_{0max}(t)$ is the distance from one maximum of oscillation to the axis and $\gamma(t)$ is the energy of electron at the same point in time. The values are taken at the maximum of oscillation since it is expected that this is the part of the trajectory that contributes more to the betatron radiation emission [2]. This comparison is presented in Fig. 2(b) as well as a synchrotron spectrum fitted so that the peak position matches that of the measured spectrum. To enable a better comparison, the three spectra were shifted vertically so that their peaks match. It can be seen that, even though the spectra are not matched, the peak position of the measured spectrum is much closer to that of the weighted spectrum than to the theoretical prediction based on the maximum values of energy and amplitude of oscillation at the last oscillation. This supports the interpretation that there is a significant influence of both the longitudinal acceleration and the distribution of energy and maximum amplitude of oscillation within the electron bunch on the final betatron spectrum.

By integrating the total energy radiated into the "virtual detector" and extrapolating this number to the total number of electrons predicted for the self-injected bunch (approximately 1.5×10^8 electrons) one obtains an estimated total radiated energy of about $1.6\mu\text{J}$. For an order of magnitude estimate of the number of photons, one can take this energy and divide it by the photon energy corresponding to the peak of the spectrum which gives a photon yield on the order of 10^9 photons.

12 GeV Single Stage Laser-Wakefield Accelerator

Assuming (future) plasma sources capable of delivering tens-of-centimeters-long plasma channels and combining them with the next generation of lasers to become available with energies on the order of 250 J, one can envision even higher energy single stage LWFA. Following this reasoning a 12 GeV single stage LWFA has been modeled and a study of the betatron radiation that could be produced by self-injected electrons in such a scenario was performed.

In the scenario modeled here, a 250 J, 800 nm wavelength laser with a peak normalized vector potential of 5.8, a duration of 110.35 fs and a $49.66 \mu\text{m}$ spot size is sent through a 21.7 cm length plasma channel with an electron density of $2.66 \times 10^{17}\text{cm}^{-3}$. The simulation parameters were chosen to obey the matching conditions in [17] and it was performed in a boosted frame with a Lorentz factor of 10. At the end of the laser propagation, the bunch of self-injected electrons had an energy spectrum exhibiting a peak at 12 GeV.

To obtain an estimate of the radiation to be expected from the betatron oscillations of the self-injected electrons in this scenario a sample of 256 trajectories randomly chosen (in the bunch) was taken and post-processed with the radiation diagnostic. The radiated energy was measured on two square detectors placed 26.5 and 52.3 cm away (see Fig. 3(a)) from the end of the plasma channel. Using the same procedure as described in the previous section the radiation angular divergence was measured to be ~ 0.6 mrad in the $x2$ and the $x3$ directions which is within the range

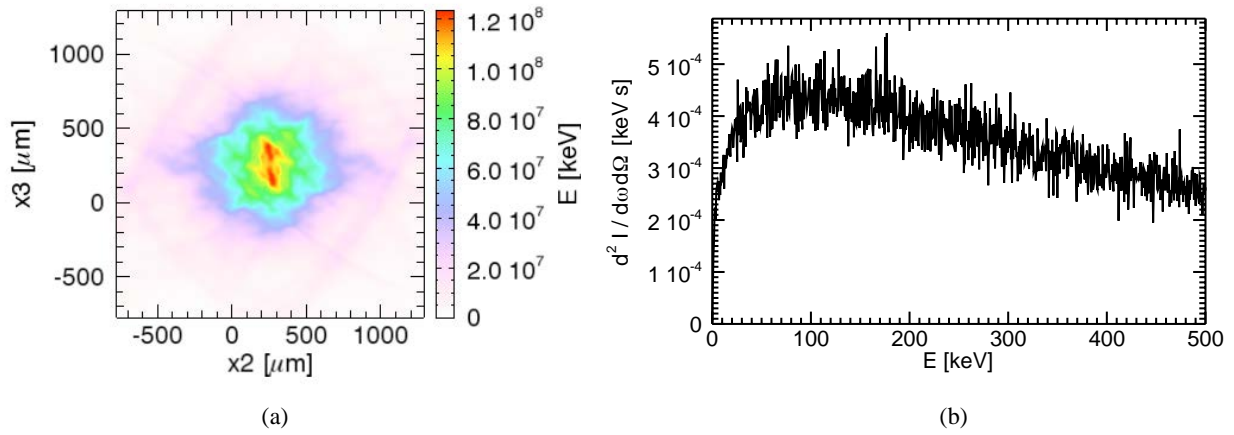


FIGURE 3. (a) Radiated energy by a sample of self-injected electrons in a 12 GeV LWFA single stage; (b) spectrum determined on-axis (at the center of the detector region).

obtained if we consider maximum and minimum values of the electron energy and of the amplitude of its betatron oscillations, which points to an angular width of the beam from ~ 12 to ~ 0.8 mrad.

To assess the spectral features of this radiation, the on-axis radiation spectrum was determined and is depicted in Fig. 3(b). The peak of this spectrum is situated approximately at the 100 keV photon energy, which is within the interval obtained by estimating the critical energy using the observed maximum and minimum values of both the energy and the amplitude of oscillations in the tracks, from ~ 72 keV to ~ 1.9 MeV. It must be stressed that the number of macroparticles considered here is considered low, but it provides a first estimation on the photon energies and total radiated energy to be expected for a future LWFA with the parameters present here. In a future publication, full spectrum calculations for a significant fraction of the self-injected bunch will be presented and discussed.

CONCLUSIONS

A diagnostic has been described that can be used as a tool for the modeling of radiative processes leveraging on the detailed information provided by PIC simulations on the individual particle trajectories, which is of special interest in cases where the emitted radiation wavelength is much shorter than the other spatial scales of the problem at study. Plasma-based accelerators are one type of problem where this difference in scales occurs, rendering this diagnostic particularly useful in the analysis of the betatron radiation.

The present radiation diagnostic was applied to the study of betatron radiation in a 1.5 GeV and a 12 GeV single laser-wakefield stages. It was observed that, as expected, the detailed properties of the electron bunch and the evolution of its energy over the laser propagation length significantly affect the betatron radiation spectrum thus clearly demonstrating the need to fully calculate the radiation of the relativistic electrons in these accelerators. This shows that this kind of radiation diagnostic combined with a PIC code can serve as valuable tool to obtain quantitative predictions on the betatron radiation in plasma-based accelerators.

ACKNOWLEDGMENTS

This work was partially supported by Fundação para a Ciência e Tecnologia (Portugal), under the grants SFRH/BD/39523/2007 and PTDC/66823/FIS/2006, and by Fundação Calouste Gulbenkian. Part of the simulations presented here were produced using the IST Cluster (IST/Portugal).

REFERENCES

1. T. Tajima and J. M. Dawson, *Phys. Rev. Letters*, **43**, 267- 270 (1979).

2. A. Rousse et al., *Phys. Rev. Letters*, **93**, 153005 (2004).
3. E. Esarey et al., *Phys. Rev. E*, **65**, 056505 (2002).
4. I. Kostyukov, S. Kiselev, and A. Pukhov, *Phys. Plasmas*, **10**, 4818 (2003).
5. K. Ta Phuoc et al., *Phys. Plasmas*, **12**, 023101 (2005).
6. S. Kneip et al., *Phys. Rev. Letters*, **100**, 105006 (2008).
7. P. Michel et al., *Phys. Rev. E*, **74**, 026501 (2006).
8. S. Wang et al., *Phys. Rev. Letters*, **88**, 135004 (2002).
9. D. K. Johnson et al., *Phys. Rev. Letters*, **97**, 175003 (2006).
10. C. B. Hededal, *Gamma-Ray Bursts, Collisionless Shocks and Synthetic Spectra*, PhD thesis (2005), arXiv:astro-ph/0506559.
11. A. G. Khachatryan et al., *New J. Physics*, **10**, 083043 (2008).
12. A. G. R. Thomas, *Phys. Rev. STAB*, **13**, 020702 (2010).
13. J. L. Martins et al., "Radiation post-processing in PIC codes" in *Harnessing Relativistic Plasma Waves as Novel Radiation Sources from Terahertz to X-Rays and Beyond*, edited by D. A. Jaroszynski and A. Rousse, Proceedings of SPIE 7359, Prague, Czech Republic, 2009, 73590V.
14. R. A. Fonseca et al., *Lec. Notes Comp. Sci.*, **2331**, 342-351 (2002).
15. R. A. Fonseca et al., *Plas. Phys. Control. Fusion*, **50**, 124034 (2008).
16. J. D. Jackson, *Classical Electrodynamics*, John Wiley & Sons, New York (1998), pp. 669 and 675.
17. W. Lu et al., *Phys. Rev. STAB*, **10**, 061301 (2007).
18. J. L. Vay, *Phys. Rev. Letters* **98**, 130405 (2007).
19. S. F. Martins et al., *Nat. Phys.* **6**, 311 - 316 (2010).